

The electrogenic $\text{Na}^+/\text{HCO}_3^-$ cotransport modulates resting membrane potential and action potential duration in cat ventricular myocytes

María C. Villa-Abrille, Martín G. Vila Petroff and Ernesto A. Aiello

Centro de Investigaciones Cardiovasculares, Facultad de Ciencias Médicas, Universidad Nacional de La Plata, La Plata 1900, Argentina

Perforated whole-cell configuration of patch clamp was used to determine the contribution of the electrogenic $\text{Na}^+/\text{HCO}_3^-$ cotransport (NBC) on the shape of the action potential in cat ventricular myocytes. Switching from Hepes to HCO_3^- buffer at constant extracellular pH (pH_o) hyperpolarized resting membrane potential (RMP) by 2.67 ± 0.42 mV ($n = 9$, $P < 0.05$). The duration of action potential measured at 50% of repolarization time (APD_{50}) was $35.8 \pm 6.8\%$ shorter in the presence of HCO_3^- than in its absence ($n = 9$, $P < 0.05$). The anion blocker SITS prevented and reversed the HCO_3^- -induced hyperpolarization and shortening of APD. In addition, no HCO_3^- -induced hyperpolarization and APD shortening was observed in the absence of extracellular Na^+ . Quasi-steady-state currents were evoked by 8 s duration voltage-clamped ramps ranging from -130 to $+30$ mV. A novel component of SITS-sensitive current was observed in the presence of HCO_3^- . The HCO_3^- -sensitive current reversed at -87 ± 5 mV ($n = 7$), a value close to the expected reversal potential of an electrogenic $\text{Na}^+/\text{HCO}_3^-$ cotransport with a $\text{HCO}_3^-:\text{Na}^+$ stoichiometry ratio of 2 : 1. The above results allow us to conclude that the cardiac electrogenic $\text{Na}^+/\text{HCO}_3^-$ cotransport has a relevant influence on RMP and APD of cat ventricular cells.

(Resubmitted 30 August 2006; accepted after revision 27 November 2006; first published online 30 November 2006)

Corresponding author E. A. Aiello: Centro de Investigaciones Cardiovasculares, Facultad de Ciencias Médicas, 60 y 120, La Plata 1900, Argentina. Email: aaiello@atlas.med.unlp.edu.ar

$\text{Na}^+/\text{HCO}_3^-$ cotransport (NBC) was first described by Boron & Boulpaep (1983) in the renal proximal tubule of the salamander, with a $\text{HCO}_3^-/\text{Na}^+$ stoichiometry of 3 : 1, which generates a net flux of negative charge across the cell membrane. In the heart, this mechanism was first reported to be present in sheep Purkinje fibres (Dart & Vaughan-Jones, 1992) and isolated guinea pig ventricular myocytes (Lagadic-Gossman *et al.* 1992) as an electroneutral transporter. However, the lack of electrogenicity of the NBC in myocardium was challenged by experiments performed in cat heart multicellular preparations (Camilión de Hurtado *et al.* 1995, 1996) and rat ventricular myocytes (Aiello *et al.* 1998) where the presence of an NBC with a $\text{HCO}_3^-/\text{Na}^+$ stoichiometry of 2 : 1 was suggested. More recently, the data proved by molecular biology supported the notion that one electroneutral (NBC3 or NBCn1) (Pushkin *et al.* 1999; Choi *et al.* 2000) and two electrogenic isoforms (NBC1b or hhNBC or NBCe1-B and NBC4 or NBCe2-c) (Choi *et al.* 1999; Pushkin *et al.* 2000; Sassani *et al.* 2002; Virkki *et al.* 2002) coexist in the myocardium. A recent work described in detail the functional diversity of the electrogenic NBC in ventricular myocytes from rat, rabbit

and guinea pig (Yamamoto *et al.* 2005). Although we have previously suggested that the electrogenic NBC contributes to the modulation of the spike-like rat action potential (AP) waveform, the participation of this transporter in the configuration of the typical prolonged cardiac AP of larger mammals is an interesting issue that remains to be studied. Thus, in this study we present evidence for the presence of an electrogenic NBC in isolated cat ventricular myocytes, and for its contribution to the modulation of resting membrane potential (RMP) and AP duration (APD).

Methods

Cell isolation

All experiments were performed in accordance with the guidelines for Animal Care of the Scientific Committee of the University of La Plata School of Medicine. Cats (body weight 3–4 kg) were anaesthetized by intraperitoneal injection of sodium pentobarbitone (35 mg (kg body weight) $^{-1}$). The chests were opened when plane three of phase III of anaesthesia was reached,

verified by the loss of the corneal reflex and appearance of slow deep diaphragmatic breathing. The hearts were quickly removed, mounted in a Langendorff apparatus and retrogradely perfused with Krebs-Henseleit solution (K-H) containing (mM): NaCl 123, KCl 4.69, CaCl₂ 1.35, NaHCO₃ 20, NaH₂PO₄ 1.2, MgSO₄ 1.2, glucose 11, pH 7.35 after gassing with 95% O₂-5% CO₂. Hearts were perfused at constant pressure for a stabilization period of 10–15 min. Single ventricular myocytes were isolated by an enzymatic dispersion technique in which hearts were perfused with nominally Ca²⁺-free K-H solution for 5 min before treatment with collagenase (74.5 u ml⁻¹, Worthington Biochemical Corp., Lakewood, NJ, USA) in Ca²⁺-free K-H solution for 45 min. The left ventricle was then removed, placed in Ca²⁺-free solution, and cut into small pieces (2 × 2 mm). After a final wash, the tissues were kept in K-H at room temperature, and single myocytes were obtained by gentle trituration.

Patch-clamp recordings

Isolated cat ventricular myocytes were placed in a recording chamber and superfused with bath solution at a flow rate of 1.5 ml min⁻¹. Only rod-shaped myocytes with clear and distinct striations and an obvious marked shortening and relaxation on stimulation were used. Experiments were performed at room temperature (20–22°C), at 30°C or at 37°C.

The nystatin perforated whole-cell configuration of the patch clamp technique (Korn *et al.* 1991) was used for voltage- and current-clamp recordings with a patch-clamp amplifier (Axopatch 200A, Axon Instruments, Union City, CA, USA). Patch pipettes were pulled with a PP-83 puller (Narishige, Tokyo, Japan) and fire-polished with a MF-83 Microforge (Narishige) to a final resistance of 0.5–1 MΩ when filled with a control pipette solution. Membrane voltage and whole-cell currents (sampling rate = 1 kHz; low pass filter = 1 kHz) were digitally recorded directly to hard disk via an analog-to-digital convertor (Digidata 1200, Axon Instruments) interfaced with an IBM clone computer running pClamp software (Axon Instruments). A pacing rate of 0.2 Hz was applied in the current-clamp recordings. Data analysis was performed with pCLAMP (Clampfit). A Ag/AgCl wire directly in contact with the extracellular solution was used as reference electrode. Since the pipette potential was nulled in external solution, all current-clamp tracings and voltage-clamp protocols required corrections for junction potential. This was accomplished by filling 20 pipettes with standard internal solution. They were then nulled in internal solution, and the difference in potential on immersion in external solution was recorded. The measured junction potential value was consistently -10 mV, and this value was used to correct all current-clamp data and voltage-clamp protocols. There were no significant

differences in the value of junction potential among all the external solutions used in the present work. For each cell, capacitive current was recorded to determine the membrane capacitance, and the currents were normalized for cell capacitance. Average cell capacitance was 126.6 ± 11.1 pF (*n* = 52).

pH_i measurements

After enzymatic isolation, myocytes were loaded with the membrane-permeant acetoxymethyl ester form of the fluorescent H⁺-sensitive indicator SNARF-1/AM. Cell suspensions (2 ml) were exposed to a final concentration of 4 μM SNARF-1/AM and 0.6% v/v DMSO. After 10 min, the myocytes were gently centrifuged for 2 min and resuspended in Hepes buffer and stored at room temperature until use. pH_i and cell length were monitored on the stage of a modified inverted microscope, as previously described (Vila Petroff *et al.* 2000). After excitation at 530 ± 5 nm, the ratio of SNARF-1/AM emission at 590 ± 5 nm to that of 640 ± 5 nm was used as a measure of pH_i according to an *in vivo* calibration, obtained from SNARF-1/AM-loaded myocytes exposed to solutions of varying pH values containing 140 mM KCl, 20 μM nigericin, 1 μM valinomycin, and 1 μM carbonyl cyanide *p*-(trifluoromethoxy)phenylhydrazone at room temperature.

Cell shortening

In some experiments, cell shortening, as an index of contractility, was measured simultaneously with the perforated-patch recordings or the pH_i measurements. Resting cell length and cell shortening were measured by a video-based motion detector (Crescent Electronics, UT, USA) and stored by software for an off-line analysis.

Solutions

The HCO₃⁻-free external solution (Hepes-buffered) contained (mM): NaCl 133, KCl 5, MgSO₄ 1.2, MgCl₂ 0.8, glucose 10, CaCl₂ 1.35, and Hepes 10, pH 7.35 with 5 mM NaOH (total Na⁺ 138 mM). The HCO₃⁻-buffered solution contained (mM): NaCl 118, KCl 5, MgSO₄ 1.2, MgCl₂ 0.8, glucose 10, CaCl₂ 1.35, Hepes 10, choline-Cl 15, and NaHCO₃ 20. The pH was titrated to 7.35 with TrisBase after gassing with 95% O₂-5% CO₂. In some experiments the extracellular solution contained 5 mM instead of 20 mM NaHCO₃, and no gassing with O₂/CO₂ was assayed. This solution was prepared fresh for each experimental day, in order to minimize the CO₂ hydration reaction. In the Na⁺-free experiments, the external NaCl was replaced completely with LiCl in both, Hepes- and HCO₃⁻-buffered solutions (in the zero Na⁺ HCO₃⁻-buffered solution, NaHCO₃ was replaced with

choline-HCO₃, LiCl was 133 mM and no choline-Cl was added). The pH of the Na⁺-free HEPES-buffered solution was titrated to 7.35 with Tris base. NaHCO₃ was replaced completely with choline-HCO₃ in the HCO₃⁻-buffered solution. The Nystatin pipette solution contained (mM): K-gluconate 130, KCl 10, NaCl 8, MgCl₂ 0.5, EGTA 1, HEPES 10, and Nystatin 0.3 mg ml⁻¹. The pH was titrated to 7.15 with KOH. NaCl was replaced with choline-Cl in the pipette solution of the Na⁺-free experiments. In all the cases, the estimated equilibrium potential for Cl⁻ was -52 mV.

Statistics

Data are expressed as mean ± S.E.M. and were compared with Student's *t* test for paired values, and repeated measures ANOVA followed by the Student-Newman-Keuls test. A value of *P* < 0.05 was considered statistically significant (two-tailed test).

Results

Figure 1A shows representative traces of cat ventricular APs before and after 1, 2, 5 and 10 min of replacing the extracellular HEPES-buffered solution (nominal HCO₃⁻-free) with a CO₂/HCO₃⁻-buffered solution (HCO₃⁻ 20 mM) at constant pH_o. The RMP hyperpolarized rapidly by approximately 3 mV in the presence of the physiological buffer. APD shortened gradually until steady-state was reached after 5 min in HCO₃⁻. Single cardiac myocytes with long APDs frequently exhibit variability in APD from one beat to another, even when paced at a constant rate, possibly

leading to a misinterpretation of our results. However, in the present work we did not detect substantial beat-to-beat APD variability, as shown in the time course of beat-to-beat APD, before and after HCO₃⁻, depicted in Fig. 1B. Thus, it seems unlikely that the changes in APD detected in the presence of HCO₃⁻ were due to beat-to-beat APD variability.

Figure 2A shows the time course of the average changes in RMP during the replacement of HEPES-buffered superfusate with HCO₃⁻-buffered solution. On average, RMP hyperpolarized 2.67 ± 0.47 mV (*n* = 9) after 5 min in the presence of HCO₃⁻. Figure 2B depicts percentage average changes in APD after 50% (APD₅₀) and 90% (APD₉₀) of repolarization time induced by the presence of HCO₃⁻ in the bath media. A significant and relevant APD₅₀ (~35%) and APD₉₀ (~25%) shortening was observed as early as 2 min after exposing the myocytes to HCO₃⁻, remaining constant afterwards during the rest of the experiment. Although without reaching statistical significance, the effect of HCO₃⁻ was more pronounced for the APD₅₀ than for the APD₉₀, possibly reflecting the higher driving force for HCO₃⁻ influx through the NBC at plateau potentials than at more repolarized potentials.

The change of a superfusate from a HEPES-buffered to a CO₂/HCO₃⁻-buffered solution induces a transient intracellular acidification due to the rapid CO₂ permeation into the cell, followed by a recovery to control values within 5–10 min after changing from HEPES to CO₂/HCO₃⁻ solutions (Dart & Vaughan-Jones, 1992, Camilión de Hurtado *et al.* 1995). Since membrane currents are sensitive to pH_i changes, these effects may partially explain the APD alterations observed in CO₂/HCO₃⁻-buffered

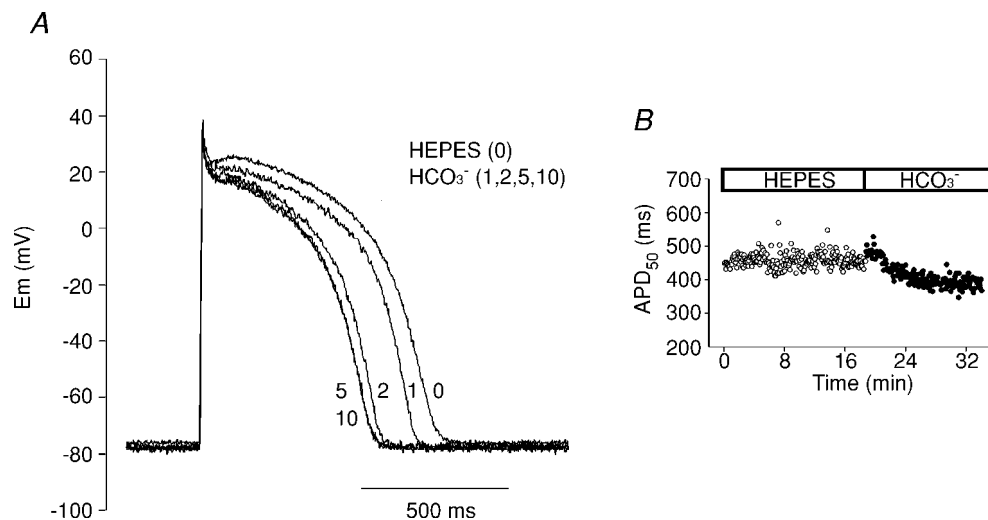


Figure 1. APD shortening after switching the extracellular solution from HEPES to HCO₃⁻-buffered solution

A, AP recordings under current-clamp mode before (HEPES) and after 1, 2, 5 and 10 min of superfusion of a cat ventricular myocyte with external HCO₃⁻. The presence of HCO₃⁻ in the external solution produced a gradual APD shortening. B, typical time course of beat-to-beat APD₅₀ measured before and after switching the extracellular solution from HEPES to HCO₃⁻.

solution. In order to evaluate the time course of pH_i changes induced by the switch from HEPES to $\text{CO}_2/\text{HCO}_3^-$ solution, we performed experiments in isolated cat myocytes in which pH_i and cell length shortening were measured simultaneously. Figure 3A shows the average changes in pH_i after the acid load induced by replacement of the HEPES-buffered superfusate with the HCO_3^- -buffered solution. An early decrease in pH_i , followed by a recovery, can be seen. Initially, CO_2 entry causes intracellular acidification but, within 2–4 min, pH_i started to recover towards control values. After 10 min, pH_i was completely recovered to values not different from those obtained before the replacement of the extracellular solution. The time course of the cell-length-shortening changes induced by the replacement of HEPES-buffered with $\text{CO}_2/\text{HCO}_3^-$ -buffered solution was associated to that of pH_i (Fig. 3B). As previously observed in cat papillary muscles (Camili3n de Hurtado *et al.* 1995), the changes in contractility were slightly delayed with respect to the changes in pH_i , suggesting that the former are secondary

to the latter, probably due to alterations in myofibrillar Ca^{2+} sensitivity and/or changes in sarcoplasmic reticulum Ca^{2+} content or fractional release (Bers, 2001).

We next recorded cell length shortening and APs simultaneously as an indirect method to evaluate whether the time course of pH_i changes observed in intact cat cardiomyocytes is similar to that of the perforated patch-clamped cat cardiomyocytes. As observed in the intact myocytes, when the superfusate was switched from HEPES to HCO_3^- -buffered solution, the perforated patch-clamped myocyte contractility transiently decreased, but within 6–8 min recovered towards control values, reaching steady-state after 8 min (Fig. 4A). These changes in contractility were faster than those observed in the epifluorescence setup, possibly due to slight differences in superfusion of the cells (i.e. different chamber sizes). However, if we consider that the changes in contractility are secondary to those of pH_i (see above), we can speculate that pH_i would be totally recovered after 6–8 min of switching the superfusate of the clamped myocytes from HEPES to $\text{CO}_2/\text{HCO}_3^-$. Thus, after 6–8 min of switching to $\text{CO}_2/\text{HCO}_3^-$, despite full recovery of pH_i , APD remained shortened (Fig. 4B), indicating that

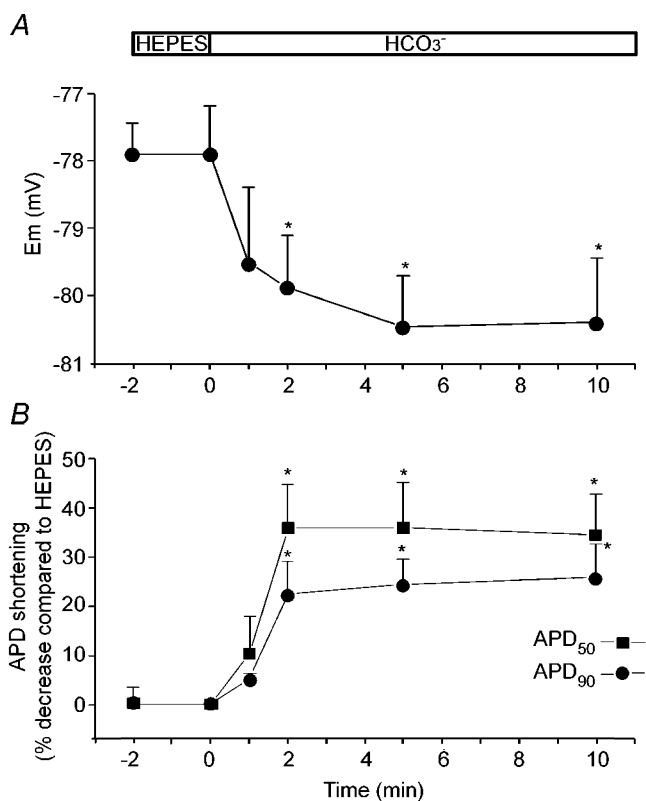


Figure 2. Hyperpolarization of RMP and shortening of the APD induced by external HCO_3^-

A, time course of the average changes in RMP after switching the superfusate from HEPES- to HCO_3^- -buffered solution ($n = 9$). *B*, time course of the percentage average changes (with respect to the value in HEPES measured immediately before the switch to HCO_3^-) in APD_{50} and APD_{90} induced by external HCO_3^- ($n = 9$). External HCO_3^- induced a slight RMP hyperpolarization and a significant and relevant shortening of the APD.

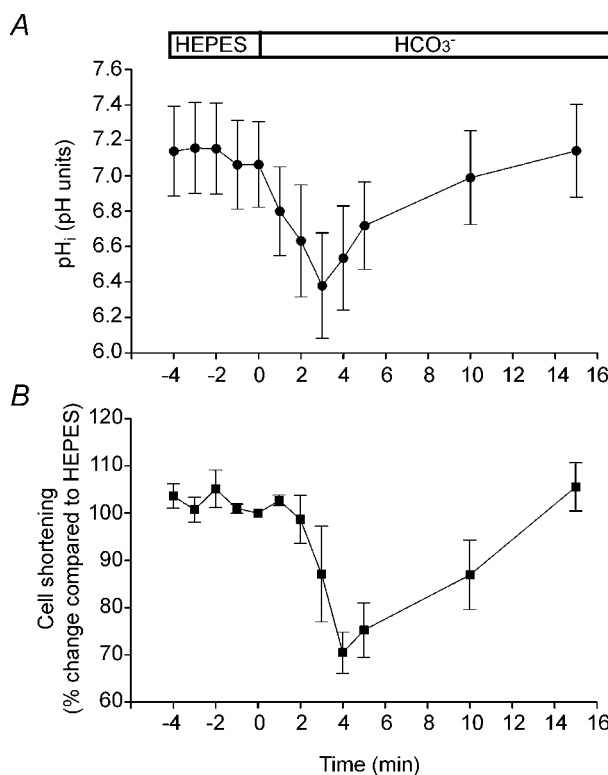


Figure 3. Simultaneous measurements of pH_i and cell shortening in the absence and presence of external HCO_3^-

A, average pH_i values obtained in five myocytes during the switch of the extracellular solution from HEPES to HCO_3^- . *B*, average cell shortening ($n = 5$, expressed as percentage change with respect to the value in HEPES measured immediately before the switch to HCO_3^-) recorded simultaneously with pH_i .

both phenomena are not related. However, taking into account that it was previously reported that acidosis causes APD lengthening (Coraboeuf *et al.* 1976; Poole-Wilson & Langer, 1975; Spitzer & Hogan, 1979), we cannot rule out the possibility that the APD shortening would have been delayed during the first minute in CO₂/HCO₃⁻ due to the transient intracellular acidification.

We next evaluated the effect on APD of a smaller concentration of HCO₃⁻ (5 mM) in the absence of CO₂ bubbling (HCO₃⁻ added to the Hepes-buffered solution), which should minimize the CO₂-induced transient intracellular acidification. Under these conditions RMP hyperpolarized from -73.8 ± 1.2 mV to -76 ± 1.2 mV (*n* = 9, *P* < 0.05) after 8 min of exposure of the myocytes to HCO₃⁻. Figure 5 shows the average values of APD₅₀ and APD₉₀ in the absence of HCO₃⁻ and after 8 min in the presence of 5 mM HCO₃⁻ in the extracellular solution. This concentration of HCO₃⁻ induced an APD₅₀ and APD₉₀ shortening of 19.3 ± 4.6% and 11.9 ± 3.8% (*n* = 9) of the values in the absence of HCO₃⁻, respectively, values

that are lower than those observed with 20 mM HCO₃⁻ (Fig. 2B). These results demonstrate that the magnitude of the APD shortening observed in HCO₃⁻ is dependent on the extracellular concentration of HCO₃⁻.

The APD shortening induced by exposure of the myocytes to 20 mM HCO₃⁻ was reversed (Fig. 6A and B) and prevented (Fig. 6C and D) by the non-specific blocker (general anionic blocker) of NBC, SITS (0.1 mM). As observed in Fig. 6, there is a tendency of APD to be slightly prolonged with SITS, but this effect did not attain statistical significance. The RMP hyperpolarization was also reversed (Hepes: -73.3 ± 2.2 mV; HCO₃⁻: -76.4 ± 2.4 mV, *P* < 0.05; HCO₃⁻ + SITS: -73.4 ± 2.3 mV; *n* = 6) and prevented by SITS (-75.3 ± 2.3 mV; Hepes + SITS: -75.6 ± 0.5 mV; HCO₃⁻ + SITS: -76.5 ± 0.5 mV; *n* = 6).

Figure 7A shows representative traces of APs recorded in Hepes zero Na⁺ and HCO₃⁻ zero Na⁺. Na⁺ was entirely replaced with Li⁺, a cation that can be carried by the Na⁺ channels (Le Guennec & Noble, 1994) and by the Na⁺/H⁺ exchanger (NHE) (Paris & Pouyssegur, 1983; Aronson, 1985), but can only minimally substitute for extracellular Na⁺ on NBC transport (Jentsch *et al.* 1985; Dart & Vaughan-Jones, 1992; Amlal *et al.* 1998; Sciortino & Romero, 1999). Changing the superfusate from Hepes- to HCO₃⁻-buffered solution in the absence of extracellular Na⁺ did not produce significant changes on the AP (Fig. 7A and B). As shown on Fig. 7B, after 10 min in the presence of HCO₃⁻ the APD₅₀ and APD₉₀ were 109.6 ± 3.9% and 107.5 ± 3.1% of the value in Hepes (*n* = 6), respectively. These results indicate that the HCO₃⁻-induced APD shortening is dependent on the presence of extracellular Na⁺, as expected for the involvement of the electrogenic NBC in this effect.

Figure 8A shows the effects of changing the extracellular superfusate from Hepes to HCO₃⁻ on steady-state

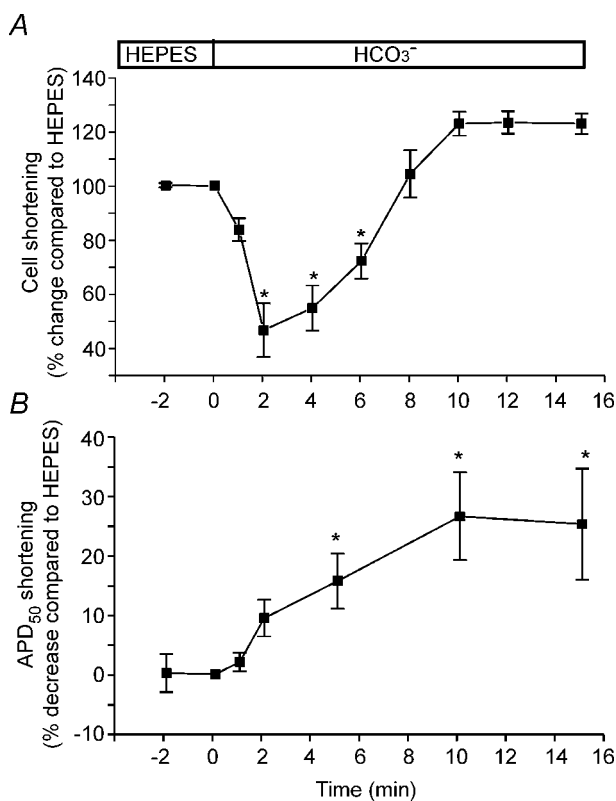


Figure 4. Simultaneous measurements of cell shortening and APD in the absence and presence of external HCO₃⁻

A, average cell shortening of seven myocytes during the switch of the extracellular solution from Hepes to HCO₃⁻. B, average APD₅₀ (*n* = 7) recorded simultaneously with cell shortening. The values were expressed as percentage change with respect to the value in Hepes measured immediately before the switch to HCO₃⁻. The HCO₃⁻-induced APD shortening remained present despite the transient decrease and postponed recovery of cell contractility.

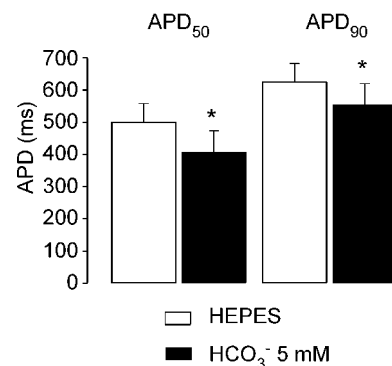


Figure 5. APD shortening induced by 5 mM HCO₃⁻

Average values of APD₅₀ and APD₉₀ in Hepes and after 8–10 min with 5 mM HCO₃⁻ in the extracellular solution (*n* = 9). This concentration of HCO₃⁻ induced an APD₅₀ and APD₉₀ shortening of 19.3 ± 4.6% and 11.9 ± 3.8% (*n* = 9) of the values in the absence of HCO₃⁻, respectively. *Significantly different from Hepes.

currents evoked by 8 s duration voltage-clamped ramps from -130 to $+30$ mV, from a holding potential of -75 mV. A novel component of an outward current was detected in the presence of HCO_3^- , consistent with an electrogenic influx of this anion. This HCO_3^- -induced outward current was cancelled by addition of SITS to the extracellular medium (Fig. 8A). Figure 8B shows the difference currents, obtained by subtraction of the current in Hepes or the current in $\text{HCO}_3^- + \text{SITS}$ to the current in HCO_3^- . The average current–voltage relationship for these two difference currents is shown in Fig. 8C. Although there was a tendency for the SITS-sensitive current to be greater than the HCO_3^- -sensitive current, the difference did not attain statistical significance. The HCO_3^- -sensitive current and the SITS-sensitive current reversed at around -85 mV (HCO_3^- -sensitive current: -87 ± 4.8 mV, $n = 7$; SITS-sensitive current: 88 ± 6 mV, $n = 7$). The reversal potential (E_{NBC}) of the NBC current (I_{NBC}) with a $\text{HCO}_3^-/\text{Na}^+$ stoichiometry of 2 : 1 was calculated with the following equation:

$$E_{\text{NBC}} = RT/F(n-1) \ln[\text{Na}^+]_i [\text{HCO}_3^-]_i^n / [\text{Na}^+]_o [\text{HCO}_3^-]_o^n$$

(Newman, 1991)

Considering that $\text{Na}_i^+ = 8$ mM, $\text{Na}_o^+ = 138$ mM, $\text{HCO}_3^-_i = 14.5$ mM ($\text{pH}_i \sim 7.2$), $\text{HCO}_3^-_o = 20$ mM

($\text{pH}_o = 7.35$) and that the experiments were performed at 20 – 22°C , E_{NBC} was calculated to be -89.4 mV, a similar value to the one measured in our experiments. Thus, these results suggest that the HCO_3^- -sensitive current and the SITS-sensitive current detected herein represents I_{NBC} .

Finally, in order to investigate the physiological implication of the electrogenic NBC in the electrical properties of cat cardiomyocytes, the impact of HCO_3^- on APD was evaluated at 30°C and 37°C . Figure 9 shows representative traces of AP before and after 10 min of switching the extracellular solution from Hepes to HCO_3^- at 30°C (Fig. 9A) or 37°C (Fig. 9C). In both cases, RMP hyperpolarization and APD shortening were observed in the presence of the physiological buffer. Average values of APD_{50} , before and after HCO_3^- , are shown in Fig. 9B (30°C) and D (37°C). On average, we detected a HCO_3^- -induced APD_{50} shortening of $14.2 \pm 1.6\%$ ($n = 8$) at 30°C and of $16.1 \pm 2.3\%$ at 37°C ($n = 4$). In Hepes, the average values of RMP were -77.5 ± 2.3 mV at 30°C and -80.7 ± 2.5 mV at 37°C ($n = 4$). After exposure of the myocytes to 10 min of HCO_3^- , RMP hyperpolarized to -81.1 ± 2.2 mV ($n = 8$, $P < 0.05$) and -84.1 ± 2.2 mV ($n = 4$, $P < 0.05$) at 30°C and 37°C , respectively. These data support the notion that the electrogenic NBC plays a

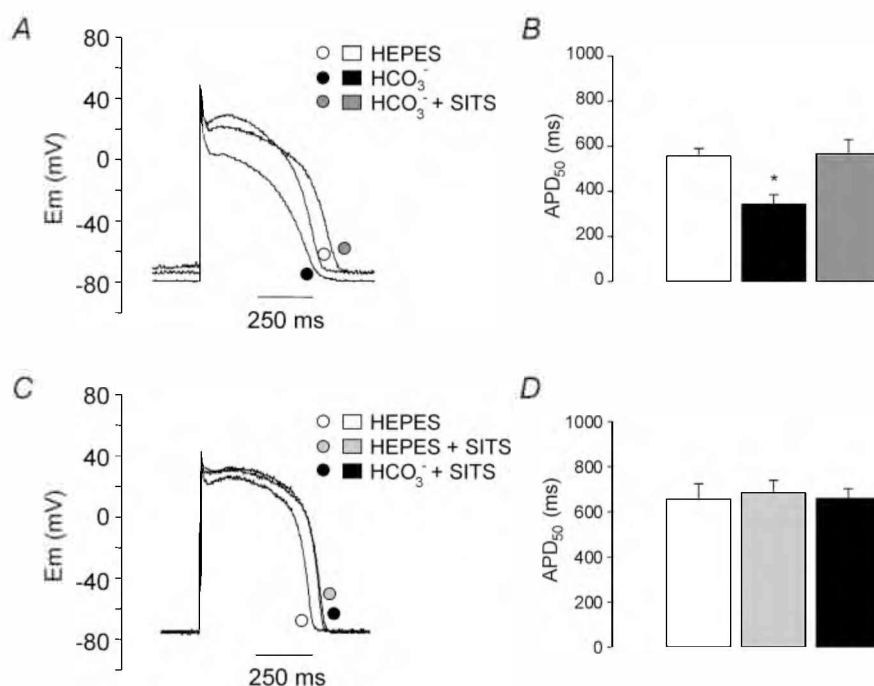


Figure 6. Effects of the anionic blocker SITS on the HCO_3^- -induced changes in APD

A, representative traces of APs recorded from a myocyte exposed successively to Hepes, HCO_3^- (10 min) and $\text{HCO}_3^- + \text{SITS}$ (0.1 mM) (10 min). B, average values of APD_{50} obtained from six myocytes subjected to the conditions of A. C, representative traces of APs recorded from a myocyte exposed successively to Hepes, Hepes + SITS (0.1 mM) (10 min) and $\text{HCO}_3^- + \text{SITS}$ (0.1 mM) (10 min). D, average values of APD_{50} obtained from six myocytes subjected to the conditions of C. The APD shortening induced by 20 mM HCO_3^- was reversed and prevented by 0.1 mM SITS. *Significantly different from Hepes.

relevant role in the electrical modelling of the ventricular AP at physiological temperatures.

Discussion

The experiments reported herein demonstrate that cat cardiac ventricular cells possess an electrogenic NBC that has a relevant impact on APD. Changing the myocytes' bathing superfusate from a HCO_3^- -free (Hepes-buffered) to a HCO_3^- -containing solution at constant pH_o , induces RMP hyperpolarization, APD shortening, and development of an outward current, consistent with the influx of HCO_3^- into the cell. These changes are sensitive to the extracellular concentration of HCO_3^- , and are blunted by anionic blockade or by sodium deprivation. Accordingly, the RMP hyperpolarization and APD shortening induced by HCO_3^- seem to have an underlying anionic current which is dependent on the presence of extracellular Na^+ , sensitive to the extracellular

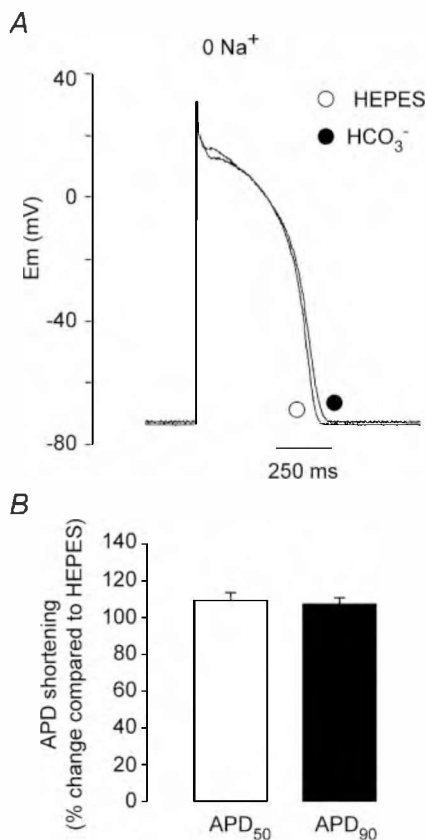


Figure 7. Effects of Na^+ deprivation on the HCO_3^- -induced changes in APD

A, representative traces of AP recordings before and after 10 min of exposure of a cat myocyte to HCO_3^- in the absence of extracellular Na^+ . No HCO_3^- -induced effects on RMP and APD were observed under these conditions. B, average change in APD_{50} and APD_{90} after 10 min in HCO_3^- zero Na^+ ($n = 4$), expressed as percentage change with respect to the value in Hepes (100%) measured immediately before the switch to HCO_3^- .

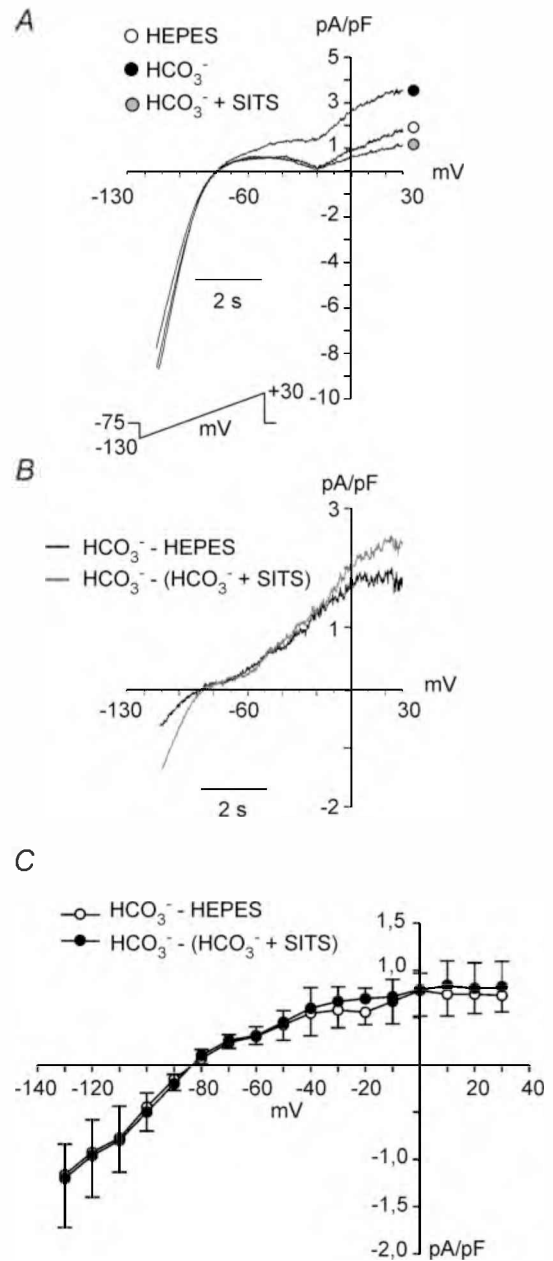


Figure 8. Effects of external HCO_3^- on steady-state currents, perforated whole-cell configuration

A, steady-state currents evoked by 8 s-duration voltage-clamp ramps ranging from -130 to $+30$ mV, from a holding potential of -75 mV, recorded from a cardiomyocyte exposed successively to external Hepes, HCO_3^- (10 min), and HCO_3^- in the presence of SITS (10 min). B, HCO_3^- -sensitive difference current ($\text{HCO}_3^- - \text{Hepes}$) and SITS-sensitive difference current ($\text{HCO}_3^- - (\text{HCO}_3^- + \text{SITS})$). C, average current–voltage relationship for the HCO_3^- -sensitive difference current ($\text{HCO}_3^- - \text{Hepes}$) ($n = 7$) and SITS-sensitive difference current ($\text{HCO}_3^- - (\text{HCO}_3^- + \text{SITS})$) ($n = 7$). These two difference currents reversed at ~ -85 mV, a value close to the expected E_{NBC} of an electrogenic NBC with a stoichiometry ratio of $2\text{HCO}_3^- : 1\text{Na}^+$.

concentration of HCO_3^- and reverses at a potential close to the estimated E_{NBC} with a $\text{HCO}_3^- : \text{Na}^+$ ratio of 2 : 1. Thus, these results strongly suggest that the relevant HCO_3^- -induced changes in RMP and APD observed in the present study are due to the activation of the electrogenic NBC present in the cardiomyocyte.

The results presented here are in agreement with early experiments performed in canine Purkinje fibres by Spitzer & Hogan (1979). The authors reported that lowering extracellular HCO_3^- at constant pH_o produced depolarization of RMP and APD lengthening. These authors suggested that these effects were due to changes in a background HCO_3^- current. In the light of the present results, it seems likely that the previously reported background HCO_3^- current of canine Purkinje fibres could have been carried by the electrogenic NBC.

Although the effects of acidosis on the cardiac action potential are relatively modest, they are manifested as a depolarization of RMP and prolongation of APD

(Coraboeuf *et al.* 1976; Poole-Wilson & Langer, 1975; Spitzer & Hogan, 1979). In our experiments, the transient acidosis caused after changing the superfusate from HEPES- to HCO_3^- -buffered solution did not seem to have significant effects on the membrane currents that control RMP or AP configuration, since in the presence of SITS or in the absence of extracellular Na^+ , exposure of the myocytes to $\text{CO}_2/\text{HCO}_3^-$ did not significantly alter RMP or APD. It is important to note that in the SITS and the zero Na^+ (replaced with Li^+) experiments, the recovery of pH_i upon changing from HEPES to $\text{CO}_2/\text{HCO}_3^-$ solution, would be partially impaired due to block of NBC, depending exclusively on the activity of the NHE. Thus, a persisting acidosis might be present at the time chosen to measure APD and RMP (10 min after changing the solutions). In order to evaluate the time course of pH_i changes in the presence of SITS or in the absence of extracellular Na^+ , we measured pH_i under these conditions. In the presence of SITS, the average

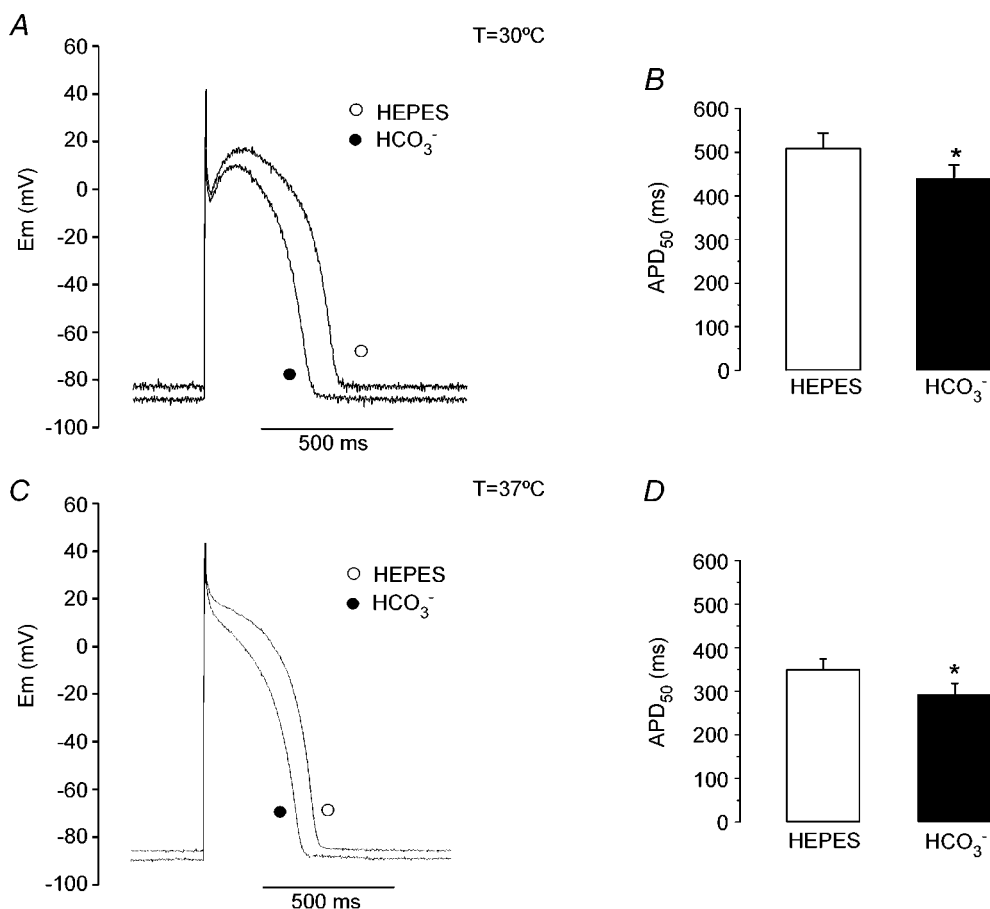


Figure 9. APD shortening induced by external HCO_3^- at 30°C and 37°C

A, AP recordings before (Hepes) and after 10 min of superfusion of a cat ventricular myocyte with external HCO_3^- at 30°C. B, average APD₅₀ ($n = 8$) measured before and after 10 min of HCO_3^- -buffered solution at 30°C. At 30°C, HCO_3^- induced an APD shortening of $14.2 \pm 1.6\%$ ($n = 8$). C, AP recordings before (Hepes) and after 10 min of superfusion of a cat ventricular myocyte with external HCO_3^- at 37°C. D, average APD₅₀ ($n = 4$) measured before and after 10 min of HCO_3^- -buffered solution at 37°C. At 37°C, HCO_3^- induced an APD shortening of $16.1 \pm 2.3\%$ ($n = 4$).

pH_i of four myocytes decreased from 7.31 ± 0.16 (Hepes) to 6.68 ± 0.23 at 3–4 min in CO₂/HCO₃⁻, recovering to 6.96 ± 0.23 at 10 min in the continuous presence of the physiological buffer. In the absence of extracellular Na⁺, the average values of pH_i of six myocytes were 7.23 ± 0.04 in Hepes, and 6.59 ± 0.10 and 6.91 ± 0.09 at 3–5 min and 10 min in CO₂/HCO₃⁻, respectively. Thus, the fact that APD in Hepes was not significantly different from that measured after 10 min in HCO₃⁻ plus SITS (Fig. 6) or HCO₃⁻ zero Na⁺ (Fig. 7), indicates that a decrease of 0.3 pH units in basal cat cardiac pH_i is not sufficient to modify the AP configuration.

The HCO₃⁻-induced hyperpolarization was small but consistent and, with the obvious cell-to-cell variability, it was present in most of the experiments performed. Moreover, just a small hyperpolarization is expected because at RMP values the driving force for HCO₃⁻ influx through the NBC with a stoichiometry ratio of 2 HCO₃⁻ : 1 Na⁺ is not large.

In the presence of external HCO₃⁻, we were able to record in isolated cat myocytes a SITS-sensitive current which reverses at approximately -85 mV. This value is very close to the estimated E_{NBC} , with a HCO₃⁻/Na⁺ stoichiometry ratio of 2 : 1. The same stoichiometry was reported for native I_{NBC} recorded in rat (Aiello *et al.* 1998; Yamamoto *et al.* 2005), rabbit and guinea pig (Yamamoto *et al.* 2005) ventricular myocytes, amphibian optic nerve and mouse cerebral astrocytes (Astion & Orkand, 1988; Brookes & Turner, 1994), leech glial cells (Deitmer & Schlue, 1989) and frog retinal epithelium (Hughes *et al.* 1989). In contrast, a stoichiometry of 3 : 1 has been estimated for mammalian proximal tubule (Boron & Boulpaep, 1983) and salamander retinal glia (Newman, 1991). This variation in stoichiometry may reflect differences in cotransporter function in different systems. A cotransporter stoichiometry of 2 : 1 in ventricular myocytes suggests that HCO₃⁻ is normally transported in an inward direction in these cells, generating an outward current that contributes to hyperpolarizing RMP and shortening APD.

An electrically silent NBC was reported to be present in sheep Purkinje fibres and isolated guinea pig myocytes, by Dart & Vaughan-Jones (1992) and Lagadic-Gossman *et al.* (1992), respectively. The authors failed to record I_{NBC} using a standard whole-cell configuration of patch-clamp technique in guinea pig ventricular myocytes (Lagadic-Gossman *et al.* 1992). However, a recent work did report the presence of I_{NBC} in guinea pig, rat and rabbit myocytes, using perforated-patch instead of standard whole-cell techniques (Yamamoto *et al.* 2005). Since our previous (Aiello *et al.* 1998) and present experiments were also performed with perforated patch, it seems mandatory that minimal altered intracellular milieu conditions (perforated-patch configuration) are necessary to detect this novel anionic current.

Yamamoto *et al.* (2005) reported that rat I_{NBC} recorded at 0 mV and 36°C was two-fold and five-fold greater than I_{NBC} recorded in guinea pig and rabbit cardiomyocytes, respectively. Thus, it seems likely that I_{NBC} is much smaller in larger animals, compared to the rat. However, in disagreement with this hypothesis, the magnitude of I_{NBC} of cat cardiomyocytes recorded herein at 0 mV and room temperature was almost two-fold higher than the one reported for rat cardiomyocytes by Yamamoto *et al.* (2005). Interestingly, if we consider the density of I_{NBC} recorded at +30 mV, cat I_{NBC} (Fig. 8) was similar to that of rat I_{NBC} (Yamamoto *et al.* 2005), due to the strong rectification of cat I_{NBC} at potentials positive to 0 mV, in comparison to rat I_{NBC} , which seems to rectify at more positive potentials (Yamamoto *et al.* 2005). Although these modest variations in the biophysical properties of I_{NBC} among these two species could be explained by the disparity in the recording temperature, it is also possible that the rectification at less positive voltages could be typical of larger mammals, since a similar phenomenon was observed in guinea pig and rabbit I_{NBC} (Yamamoto *et al.* 2005). Although both electrogenic isoforms of NBC, NBC1 and NBC4, were reported to be present in normal human heart (Choi *et al.* 1999; Pushkin *et al.* 2000), no studies have yet shown the presence of native I_{NBC} in human cardiomyocytes. Thus, the evaluation of human cardiac I_{NBC} and its influence on APD and RMP represents a relevant matter to be addressed in the near future.

We presented herein that the HCO₃⁻-induced APD shortening was also present at physiological temperatures. However, although the NBC activity was reported to be slowed by reduced temperature (Ch'en *et al.* 2003), the magnitude of the HCO₃⁻-induced APD shortening at physiological temperatures was not greater, but actually smaller, than at room temperature. Although we do not have data that can certainly explain the reason for this difference, we can speculate that the expected decrease in membrane resistance and increase in other ionic currents at higher temperatures could account for the smaller effect of I_{NBC} on APD.

Yamamoto *et al.* (2005) have shown that the cardiac NBC activity is associated with a net Na⁺ influx to the cell. After the acidification induced by ischaemia, Na⁺-coupled acid extrusion during ischaemia and/or reperfusion contributes to net H⁺ efflux. The associated Na⁺ entry may contribute to a rise in [Na⁺]_i and therefore Ca²⁺ overload via Na⁺/Ca²⁺ exchange. Vandenberg *et al.* (1993) showed that the NBC contributes to about 20% to the total pH_i recovery during reperfusion. Schafer *et al.* (2000) demonstrated that during reoxygenation of rat myocytes exposed to 70 min of anoxia, the NBC also plays an important role in pH_i recovery (approximately 50% of the total pH_i recovery). Furthermore, these authors showed that the calcium oscillations that cause hypercontracture of the cells were diminished by DIDS, a

blocker of the NBC (Schafer *et al.* 2000). More recently, Khandoudi *et al.* (2001) have shown in perfused rat hearts that the presence of a selective antibody against cardiac NBC1b significantly improved the post-ischaemic functional recovery. These authors also showed that NBC1b but not NBC3 protein expression in human myocardium from patients with heart failure was markedly increased in comparison to control hearts (Khandoudi *et al.* 2001). In addition, an upregulation of NBC1 mRNA and protein was reported to be present after myocardial infarction in the rat heart (Sandmann *et al.* 2001). Finally, since the NBC1b is a Na^+ -loading mechanism, the overexpression of this transporter might contribute to increase the incidence of arrhythmias in the failing heart (Verdonck *et al.* 2003). Accordingly, the contribution of I_{NBC} to the shape of the AP in pathophysiological states represents an interesting forthcoming issue to be resolved.

In summary, the present study demonstrates the presence of an electrogenic NBC in isolated cat ventricular myocytes that participates in the modulation of RMP and APD. These effects originate from the presence of a SITS-sensitive outward current that can be seen only when HCO_3^- and Na^+ are present in the media. Although HCO_3^- is the physiological buffer, HCO_3^- -buffered solutions are not usually employed in patch-clamp experiments, masking the observation of these effects. From these results it is clear that I_{NBC} should be considered as part of the currents contributing to the configuration of the cardiac AP.

References

- Aiello EA, Vila Petroff MG, Mattiazzi AR & Cingolani HE (1998). Evidence for an electrogenic $\text{Na}^+/\text{HCO}_3^-$ symport in rat cardiac myocytes. *J Physiol* **512** *1*, 137–148.
- Amlal H, Wang Z, Burnham C & Soleimani M (1998). Functional characterization of a cloned human kidney $\text{Na}^+:\text{HCO}_3^-$ cotransporter. *J Biol Chem* **273**, 16810–16815.
- Aronson PS (1985). Kinetic properties of the plasma membrane Na^+-H^+ exchanger. *Annu Rev Physiol* **47**, 545–560.
- Astion MK & Orkand RK (1988). Electrogenic $\text{Na}^+/\text{HCO}_3^-$ cotransport in neuroglia. *Glia* **1**, 355–357.
- Bers DM (2001). Cardiac inotropy and Ca mismanagement. In *Excitation-Contraction Coupling and Cardiac Contractile Force*, 2nd edn, ed. Bers DM, pp. 273–331. Kluwer Academic Publishers, Dordrecht.
- Boron WF & Boulpaep EL (1983). Intracellular pH regulation in the renal proximal tubule of the salamander. *J General Physiol* **8**, 53–94.
- Brookes N & Turner RJ (1994). K^+ -induced alkalinization in mouse cerebral astrocytes mediated by reversal of electrogenic $\text{Na}^+-\text{HCO}_3^-$ cotransport. *Am J Physiol Cell Physiol* **267**, C1633–C1640.
- Camili3n de Hurtado MC, Alvarez BV, P3rez NG & Cingolani HE (1996). Role of an electrogenic $\text{Na}^+/\text{HCO}_3^-$ cotransport in determining myocardial pH_i after an increase in heart rate. *Circ Res* **79**, 698–704.
- Camili3n de Hurtado MC, P3rez NG & Cingolani HE (1995). An electrogenic sodium-bicarbonate cotransport in the regulation of myocardial intracellular pH. *J Mol Cell Cardiol* **27**, 231–242.
- Ch'en FFT, Dilworth E, Swietach P, Goddard RS & Vaughan-Jones RD (2003). Temperature dependence of Na^+-H^+ exchange, $\text{Na}^+-\text{HCO}_3^-$ co-transport, intracellular buffering and intracellular pH in guinea-pig ventricular myocytes. *J Physiol* **552**, 715–726.
- Choi I, Aalkjaer C, Boulpaep EL & Boron WF (2000). An electroneutral sodium/bicarbonate cotransporter NBCn1 and associated sodium channel. *Nature* **405**, 571–575.
- Choi I, Romero MF, Khandoudi N, Bril A & Boron WF (1999). Cloning and characterization of a human electrogenic $\text{Na}^+-\text{HCO}_3^-$ cotransporter isoform (hhNBC). *Am J Physiol Cell Physiol* **276**, C576–C584.
- Coraboeuf E, Deroubaix E & Hoerter J (1976). Control of ionic permeabilities in normal and ischemic heart. *Circ Res* **38**, 192–198.
- Dart C & Vaughan-Jones RD (1992). $\text{Na}^+-\text{HCO}_3^-$ symport in the sheep cardiac Purkinje fibre. *J Physiol* **451**, 365–385.
- Deitmer JW & Schlue WR (1989). An inwardly directed electrogenic sodium-bicarbonate co-transport in leech glial cells. *J Physiol* **411**, 179–194.
- Hughes BA, Adorante JS, Miller SS & Lin H (1989). Apical electrogenic NaHCO_3 cotransport. A mechanism for HCO_3^- absorption across the retinal pigment epithelium. *J Gen Physiol* **94**, 125–150.
- Jentsch TJ, Schill BS, Schwartz P, Matthes H, Keller SK & Wiederholt M (1985). Kidney epithelial cells of monkey origin (BSC-1) express a sodium bicarbonate cotransport. Characterization by $^{22}\text{Na}^+$ flux measurements. *J Biol Chem* **260**, 15554–15560.
- Khandoudi N, Albadine J, Robert P, Krief S, Berrebi-Bertrand I, Martin X, Bevensee MO, Boron WF & Bril A (2001). Inhibition of the cardiac electrogenic sodium bicarbonate cotransporter reduces ischemic injury. *Cardiovasc Res* **52**, 387–396.
- Korn SJ, Marty A, Connor JA & Horn R (1991). Perforated patch recording. *Meth Neurosciences* **4**, 364–373.
- Lagadic-Gossman DK, Buckler J & Vaughan-Jones RD (1992). Role of bicarbonate in pH recovery from intracellular acidosis in the guinea-pig ventricular myocyte. *J Physiol* **458**, 361–384.
- Le Guenneq JV & Noble DJ (1994). Effects of rapid changes of external Na^+ concentration at different moments during the action potential in guinea-pig myocytes. *J Physiol* **478**, 493–504.
- Newman EA (1991). Sodium-bicarbonate cotransport in retinal glia of the salamander. *J Neuroscience* **11**, 3972–3983.
- Paris S & Pouyssegur J (1983). Biochemical characterization of the amiloride sensitive Na^+/H^+ antiport in Chinese hamster lung fibroblasts. *J Biol Chem* **258**, 3503–3508.
- Poole-Wilson PA & Langer GA (1975). Effect of pH on ionic exchange and function in rat and rabbit myocardium. *Am J Physiol* **229**, 570–581.
- Pushkin A, Abuladze N, Lee I, Newman D, Hwang J & Kurtz I (1999). Cloning, tissue distribution, genomic organization, and functional characterization of NBC3, a new member of the sodium bicarbonate cotransporter family. *J Biol Chem* **274**, 16569–16575.

- Pushkin A, Abuladze N, Newman D, Lee I, Xu G & Kurtz I (2000). Cloning, characterization and chromosomal assignment of NBC4, a new member of the sodium bicarbonate cotransporter family. *Biochim Biophys Acta* **1493**, 215–218.
- Sandmann SYuM, Kaschina E, Blume A, Bouzinova E, Aalkjaer C & Unger T (2001). Differential effects of angiotensin AT₁ and AT₂ receptors on the expression, translation and function of the Na⁺–H⁺ exchanger and Na⁺–HCO₃[–] symporter in the rat heart after myocardial infarction. *J Am Coll Cardiol* **37**, 2154–2165.
- Sassani P, Pushkin A, Gross E, Gomer A, Abuladze N, Dukkipati R, Carpenito G & Kurtz I (2002). Functional characterization of NBC4: a new electrogenic sodium-bicarbonate cotransporter. *Am J Physiol Cell Physiol* **282**, C408–C416.
- Schafer C, Ladilov YV, Siegmund B & Piper HM (2000). Importance of bicarbonate transport for protection of cardiomyocytes against reoxygenation injury. *Am J Physiol Heart Circ Physiol* **278**, H1457–H1463.
- Sciortino CM & Romero MF (1999). Cation and voltage dependence of rat kidney electrogenic Na⁺–HCO₃[–] cotransporter, rNBC, expressed in oocytes. *Am J Physiol Renal Physiol* **277**, F611–F623.
- Spitzer KW & Hogan PM (1979). The effects of acidosis and bicarbonate on action potential repolarization in canine cardiac Purkinje fibers. *J Gen Physiol* **73**, 199–218.
- Vandenberg JI, Metcalfe JC & Grace AA (1993). Mechanisms of pH_i recovery after global ischemia in the perfused heart. *Circ Res* **72**, 993–1003.
- Verdonck F, Volders PGA, Vos MA & Sipido KR (2003). Intracellular Na⁺ and altered Na⁺ transport mechanisms in cardiac hypertrophy and failure. *J Mol Cell Cardiol* **35**, 5–25.
- Vila Petroff MG, Aiello EA, Palomeque J, Salas MA & Mattiazzi AR (2000). Subcellular mechanisms of the positive inotropic effect of angiotensin II in cat myocardium. *J Physiol* **529**, 189–203.
- Virkki LV, Wilson DA, Vaughan-Jones RD & Boron WF (2002). Functional characterization of human NBC4 as an electrogenic Na⁺–HCO₃[–] cotransporter (NBCe2). *Am J Physiol Cell Physiol* **282**, C1278–C1289.
- Yamamoto T, Swietach P, Rossini A, Loh SH, Vaughan-Jones RD & Spitzer KW (2005). Functional diversity of electrogenic Na⁺–HCO₃[–] cotransport in ventricular myocytes from rat, rabbit and guinea pig. *J Physiol* **562**, 455–475.

Acknowledgements

This work was partly supported by a grant from the Agencia Nacional de Promoción Científica y Tecnológica (PICT 25495 to E.A.A.). The authors wish to thank Mónica Rando for excellent technical assistance.